DOI: https://doi.org/10.57233/ijsgs.v12i1.1060 ISSNp: 2488-9229; ISSNe: 3027-1118

IJSGS FUGUSAU VOL. 12(1) WEBSITE: https://fugus-

INTERNATIONAL JOURNAL OF SCIENCE FOR GLOBAL SUSTAINABILITY
(A PUBLICATION OF FACULTY OF SCIENCE, FEDERAL UNIVERSITY GUSAU, NIGERIA)

Mineralogical Studies of the Underlying Rocks around Jiko Abandoned Mine Site, North-Central Nigeria

Hammed Rasheed[1,2,*]

[1]Department of Geology, Federal University of Technology, Minna, Nigeria
[2]Department of Geology, University of Ibadan, Nigeria
***Corresponding Author:** geohammed2016@gmail.com

ABSTRACT

The mineralogical characterisation of crystalline basement rocks is fundamental to constraining protolith affinity and geological and geochemical processes in mining-impacted terrains. This study presents the first integrated X-ray diffraction (XRD) and transmitted-light petrographic investigation of basement rocks underlying the Jiko abandoned mine site, North-Central Nigeria, within the Kusheriki schist belt of the Nigerian Basement Complex. The aim is to establish a mineralogical framework for interpreting rock evolution and its implications for geochemical behaviour. Six representative rock samples, ranging from fresh to moderately altered, were systematically collected and analysed using powder XRD (Cu-Kα radiation; 5–75° 2θ) for phase identification and optical petrography for textural and paragenetic relationships. XRD results indicate a dominant primary mineral assemblage of quartz, phlogopite, and albite, with accessory ilmenite occurring in Ti–Fe-enriched samples and secondary goethite and haematite preferentially developed in altered rocks. Petrographic analysis reveals two principal domains: (i) a schistose domain characterised by aligned mica laths, quartz ribbons, undulose extinction, and incipient feldspar sericitisation; and (ii) a gneissic to altered domain defined by compositional banding, granoblastic textures, fractured and oxidised micas, feldspar turbidity, and pervasive Fe-oxide precipitation along fractures and grain boundaries. These mineralogical and textural relationships indicate that the Jiko basement rocks represent low- to medium-grade metamorphic lithologies, consistent with phlogopite-quartz-albite schists and associated gneisses derived from predominantly pelitic to semi-pelitic protoliths, with local Fe-Ti enrichment. A progressive weathering sequence is established, transitioning from primary quartz-phlogopite ± albite ± ilmenite assemblages through early-stage mica degradation and feldspar alteration to advanced formation of goethite and haematite along structurally controlled fluid pathways. This evolution highlights the critical role of deformation fabric and fracture networks in facilitating fluid ingress and mineral transformation. The study demonstrates that basement mineralogy, coupled with microstructural controls, governs secondary mineral development and provides a robust framework for interpreting trace-element mobilisation and environmental risk in mining-affected basement terrains. It is recommended that future work integrates mineralogical data with in-situ microanalysis (e.g., SEM-EDS, EPMA) and isotopic tracing to better resolve mineral-geochemical linkages and element provenance. These findings are transferable to comparable Pan-African basement settings and contribute to a process-based understanding of mineralogical evolution in tropical weathering environments.

Keywords: Jiko abandoned mine site, Basement Complex mineralogy, Petrography, Phlogopite-quartz-albite assemblage, Tropical weathering processes

1.0 INTRODUCTION

The systematic mineralogical characterisation of crystalline basement rocks constitutes the essential first step in understanding their protoliths (i.e., precursor minerals) and provides insights into the geochemical behaviour of trace elements, the mechanisms of secondary mineral formation, and the broader environmental implications of rock weathering in mining-affected landscapes (Akinola &Olorun, 2021). In Precambrian basement terrains such as the Nigerian Basement Complex, the diversity of primary mineral assemblages, ranging from mica-rich schists and feldspathic gneisses to oxide-bearing metamorphic rocks, determines both the nature of secondary weathering products and the intrinsic geochemical fingerprint of any overlying environmental media such soils and surface waters (Lukman *et al.* 2024). Establishing this primary mineralogical framework therefore underpins any scientifically credible assessment of whether elevated trace element concentrations observed in surficial geochemical environments reflect lithogenic sources or anthropogenic contamination.

X-ray diffraction (XRD) provides the definitive technique for bulk mineral phase identification in polycrystalline rocks, enabling unambiguous determination of mineral species from their characteristic d-spacings and diffraction peak positions (Ali *et al.*, 2022). When combined with optical petrography of thin sections, which reveals grain-scale textural relationships, fabric development, alteration textures, and mineral paragenesis that XRD alone cannot resolve, the two methods together yield a comprehensive and mutually corroborating mineralogical dataset (Ali *et al.*, 2022; Oluyede *et al*., 2021; Falana, 2025). Such integrated approaches have been employed successfully in characterising basement geology across the Nigerian schist belts, including kyanite-bearing metapelites of the Kusheriki Schist Group (Muhammed *et al.*, 2018) and mica-rich assemblages along the BirninGwari and Zungeru schist belts (Adepoju *et al*., 2021; Oluyede *et al.*, 2021).

The Jiko abandoned mine site, situated within Munya Local Government Area, Niger State, occupies a segment of the Pan-African Basement Complex characterised by phlogopite-bearing schists, gneissic lithologies, and structurally controlled quartz-vein mineralisation (Ahmed *et al.*, 2020). Artisanal and small-scale gold mining (ASM) has operated at this site for several decades, involving excavation, crushing, and alluvial panning of mineralised

DOI: https://doi.org/10.57233/ijsgs.v12i1.1060 ISSNp: 2488-9229; ISSNe: 3027-1118

basement material. Despite growing documentation of elevated metal concentrations in soils and surface waters at the site (Rasheed *et al.*, 2026a, in press), no systematic study has yet characterised the primary and secondary mineral assemblages of the host rocks using XRD and optical petrography. The absence of this mineralogical baseline represents a significant gap in understanding whether observed contamination (Rasheed *et al.*, 2026b, in press) reflects lithogenic (or geogenic) mineral sources or is a product of anthropogenically-induced ASM activities alone.

This study therefore presents the first integrated XRD and optical petrographic characterisation of the basement rocks at the Jiko abandoned mine site. The specific objectives are: (i) to identify and describe the primary rock-forming mineral assemblages using powder XRD, with detailed peak and d-spacing analysis; (ii) to characterise mineral textures, fabric types, alteration phases, and paragenetic relationships using transmitted-light optical petrography of polished thin sections; and (iii) to interpret the nature and significance of the identified mineral assemblages in terms of rock type, metamorphic grade, weathering state, and environmental geochemical relevance. Thus, the study aims to provide a robust and reproducible mineralogical reference dataset for the Jiko basement, directly supporting future investigations of metal mobility, environmental risk assessment, and site remediation planning in this and comparable abandoned mine sites across North-Central Nigeria.

2.0 STUDY AREA AND GEOLOGICAL SETTING

2.1 Location and Access

The study area (Figure 1) is centred on Jiko Village in Munya Local Government Area (LGA), Niger State, North-Central Nigeria, within the Minna Sheet 164 of the Nigerian Geological Survey Agency (NGSA). The site lies approximately 70 km northwest of Minna, in the vicinity of the Niger-Kaduna State boundary, between latitudes 9°39′25.6″N and 9°42′26.2″N and longitudes 6°48′12.2″E to 6°49′23.0″E. Access is via an unpaved laterite road branching from the Minna-Mutum Daya road corridor, supplemented by narrow footpaths that traverse subsistence farmland, drainage channels, and the mine working areas. Numerous open mine pits, spoil heaps, quartz-cobble dumps, alluvial panning sites along stream banks, and exposed rock scarps are distributed throughout the study area, providing clear field evidence of both active and legacy artisanal gold mining operations.

2.2 Climate, Topography, and Drainage

The Jiko area lies within the Sudan-Guinea Savanna transition zone and experiences a tropical wet-dry climate with clearly defined rainy (April-October) and dry (November-March) seasons. Rainfall peaks in August-September, while the dry season is accompanied by the north-easterly Harmattan winds. The terrain is gently undulating, with low-relief hills rising above broad fluvial plains connected to the River Niger catchment. Sampled outcrops are generally at elevations exceeding 350 m above the sea level (ASL), ranging from 372 to 398 m. The drainage system consists of small seasonal streams and wider channels active during the rains, exposing fresh and moderately weathered bedrock along stream banks and valley walls. These exposures provided the primary sites for rock sample collection.

2.3 Regional and Local Geology

The Nigerian Basement Complex underlies the entire study area and forms part of the broad Precambrian metamorphic and igneous terrane that extends across most of western sub-Saharan Africa (Ekeleme *et al.*, 2024; Yusuf *et al.*, 2026). The complex is subdivided into four major lithotectonic units: the Migmatite-Gneiss Complex (MGC), the Schist Belts, the Pan-African Older Granites, and undeformed Acid and Basic Dykes (Ekeleme *et al.*, 2024). The Jiko area falls within the schist belt province, specifically the KusherikiPsammite Formation that forms part of the Minna Sheet 164 Precambrian basement. The schist belts of north-central Nigeria trend predominantly NE-SW and are characterised by low- to medium-grade metamorphic rocks including mica schists, quartzites, quartz-kyanite schists, and subordinate Banded Iron Formations (Salawu *et al.*, 2021; Oluyede *et al.*, 2021; Fagbohun*et al.*, 2025). These belts are interpreted as reactivated passive continental margin sequences reworked during Pan-African orogenesis at approximately 600 Ma (Ojo *et al.*, 2020). Structurally controlled quartz-vein systems, many of which carry auriferous and polymetallic mineralisation, are hosted within and along the margins of the mica schist and gneissic units.

Locally, the bedrock of the Jiko area comprises two principal lithological assemblages: (i) phlogopite-quartz schists displaying a strong NE-SW trending foliation that dips moderately to steeply to the south-east or north-east depending on structural position, and (ii) quartz-feldspar-biotite gneisses with well-developed compositional banding. Both assemblages are cross-cut by white to milky quartz veins of variable dimensions and by rare mafic dykes. At several locations, the contact between the schistose and gneissic units is gradational over several metres, suggesting they represent part of a single progressively deformed and partially differentiated basement sequence rather than distinct lithostratigraphic formations.

DOI: https://doi.org/10.57233/ijsgs.v12i1.1060 ISSNp: 2488-9229; ISSNe: 3027-1118

IJSGS FUGUSAU VOL. 12(1) WEBSITE: https://fugus-

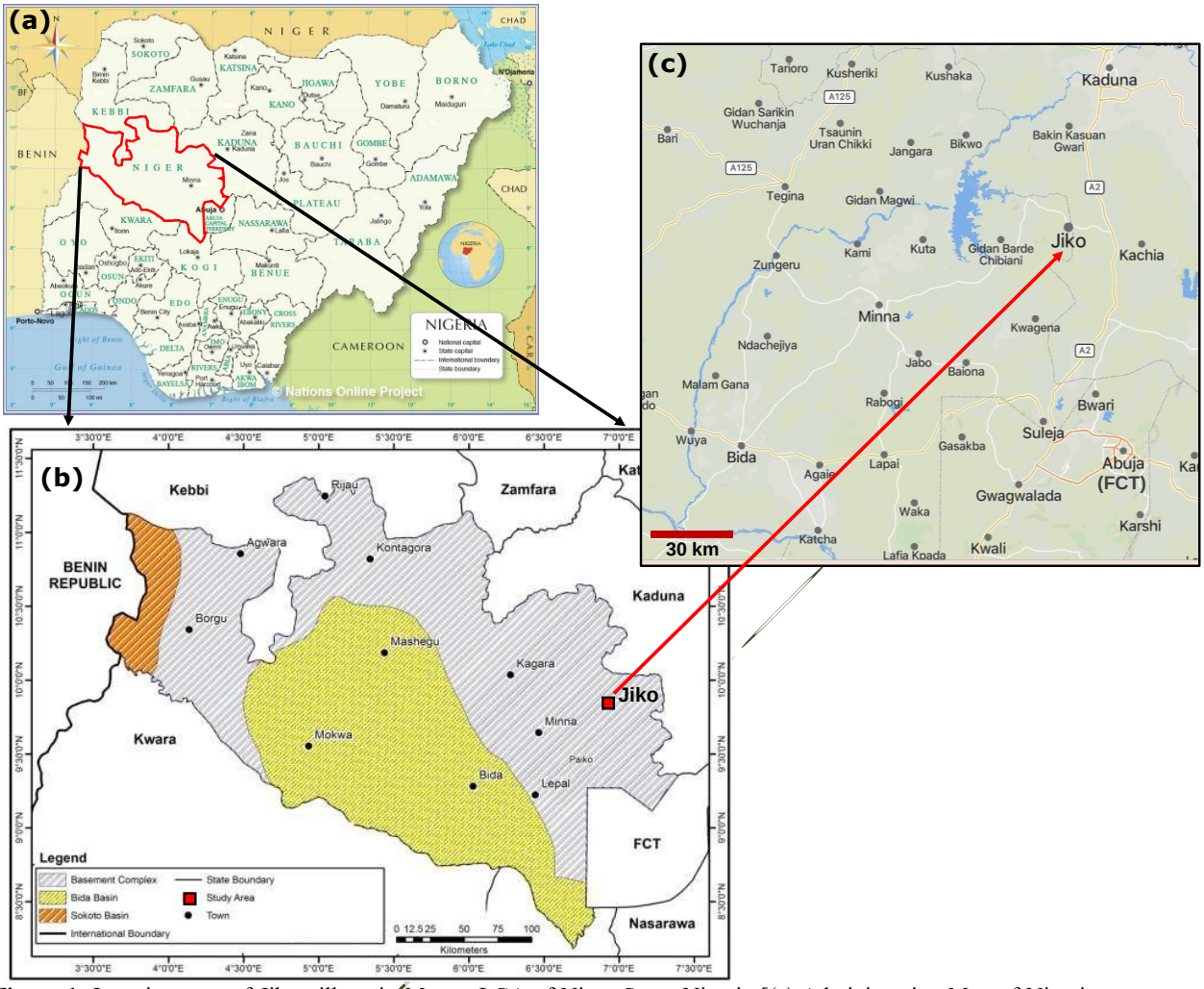

Figure 1: Location map of Jiko village in Munya LGA of Niger State, Nigeria [(a) Administrative Map of Nigeria (https://www.nationsonline.org/oneworld/map/nigeria-administrative-map.htm); (b) GeologicalMap of Niger State showing the Study Area (Modified after Ahmed *et al.,* 2020); and (c) Jiko village on Mapcarta (https://mapcarta.com/33243376)].

2.4 Field Observations and Hand Specimen Descriptions

Systematic field observations were conducted across six sampling points distributed across the principal outcrop areas. The two dominant rock assemblages - the schistose rocks and the gneissic to altered rocks - were carefully described in hand specimen at each station.

2.4.1 Schistose Rocks (Samples R1, R2, and R4)

The schistose rocks are the most widespread lithology in the study area and form low, rounded outcrops and slabby pavement exposures along hillslopes and stream banks. In fresh hand specimens, they are medium to dark grey in overall colour, with a metallic silky lustre imparted by the abundant aligned mica flakes that define the principal foliation (S_1). The foliation is well-developed and pervasive, dipping generally between 40° and 65° to the south-east with strikes broadly NE-SW. Compositionally, the rocks show a clear segregation into thin alternating mica-rich layers (~1–5 mm thick, darker grey to silvery) and quartz-rich domains (~2–8 mm thick, pale grey to white). This millimetre-scale lithological banding gives the fresh rock a subtle striped appearance when viewed along strike.

The mica fraction, which comprises the dominant mineral constituent by volume, occurs as small to medium-sized platy crystals (~0.5-3 mm) aligned strictly parallel to the foliation. Individual crystals have a bronze to pale brown tint in strong oblique light. Quartz forms lustrous, sub-vitreous, pale grey to white granular masses and thin lenticular ribbons (quartz eyes) of ~2-15 mm length, oriented parallel to the foliation. Feldspar is present but not conspicuous in hand specimen, occurring as pale grey to dull white irregular granular aggregates interspersed with mica and quartz. The overall texture is lepidoblastic-granoblastic.

Quartz veins of white to milky-white colour and ranging from 3 mm to approximately 2 cm in width cut the schistosity at angles of approximately 10° to 30°, representing a later stage of fluid infiltration along structurally favourable planes. At sample locality R2, the

DOI: https://doi.org/10.57233/ijsgs.v12i1.1060 ISSNp: 2488-9229; ISSNe: 3027-1118

foliation surfaces show localised pale yellow to rusty-brown staining, indicating incipient iron oxide precipitation from weathering fluids migrating along cleavage planes. Sample R4 is the freshest of the schistose specimens; its foliation surfaces are clean, metallic, and display a characteristic silky sheen, with no visible oxidation products. The rock is notably competent and breaks with a clean fracture parallel to schistosity.

2.4.2 Gneissic and Altered Rocks (Samples R2B, R3, and R3B)

The gneissic and altered rocks crop out as larger, more massive outcrops and boulders, particularly in the central and northern parts of the study area. They are coarser grained than the schistose varieties and display a well-defined compositional banding (gneissic banding) rather than a platy schistosity. Bands alternate between pale grey to white felsic layers (quartz + feldspar-dominated, ~5-15 mm thick) and dark grey to black mafic layers (biotite-phlogopite-dominated, 3-10 mm thick), imparting a striking striped appearance to outcrop faces.

In fresh to moderately weathered hand specimens, the felsic layers have a granular, sugar-like texture and a dull to sub-vitreous lustre, while the mafic layers retain a clearly platy character but with more compacted, less individually distinct mica crystals compared to the schistose rocks. Quartz in the gneissic rocks tends to form equant grains and small aggregates rather than the elongate ribbons typical of the schists. Feldspar is more visually prominent in the gneissic rocks, appearing as white to pale pink tabular grains ~1-4 mm in size within the felsic bands, but occasionally greater than 5 mm.

Sample R3 is dark grey and notably heavier than the other specimens when held in hand, consistent with a higher content of dense Ti-Fe-bearing minerals confirmed later by XRD as ilmenite. Its surface has a faint metallic sub-lustre, and the mica component appears darker and more opaque than in the schistose counterparts, suggesting a more Fe-rich biotite. Quartz in R3 forms both small grains and coarser lenticular masses up to 3 cm, some of which show a milky, vein-like character. Sample R3B and R2B are the most strongly altered specimens in the collection. Their surfaces show pervasive orange-yellow to deep reddish-brown limonitic and haematitic coatings, particularly on fracture faces and along the contacts between felsic and mafic bands. Scraping these surfaces with a geological hammer reveals a slightly fresher grey to brown interior, confirming that oxidation is a surficial and fracture-controlled process rather than a complete volumetric transformation of the rock. Several fracture surfaces in R3B display dark brown to black botryoidal and sub-colloform coatings consistent with goethite and haematite precipitation, phases subsequently confirmed by XRD analysis.

3. MATERIALS AND METHODS

3.1 Rock Sampling

Field investigations were conducted at Jiko Village between 15 April and 10 June 2019. Geological mapping, outcrop description, and sample collection were undertaken at six locations distributed across the principal lithological exposures. Samples were collected from relatively fresh rock surfaces using a geological hammer and chisel, taking care to avoid highly weathered rinds where present by splitting samples to expose fresh interiors. Each sample was wrapped in brown paper, placed in a labelled polythene bag, and transported to the National Geosciences Research Laboratories (NGRL) of Nigerian Geological Survey Agency (NGSA), Kaduna, for XRD analysis. Sub-samples were also transported to the NGSA Petrology Laboratory for thin-section preparation. Geographic coordinates and elevations at each sampling point were recorded using a handheld GPS receiver and are presented alongside field descriptions in Table 1.

3.2 Powder X-Ray Diffraction (XRD)

Bulk mineralogical characterisation was carried out by powder X-ray diffraction at the National Geosciences Research Laboratories (NGRL), NGSA, Kaduna, using a PANalytical Empyrean series diffractometer fitted with a Cu anode X-ray tube. The analytical setup, confirmed from the instrument scan parameter records of the analysed samples, employed a generator setting of 40 mA and 45 kV, with Cu Kα radiation ($K\alpha_1$ = 1.54060 Å, $K\alpha_2$ = 1.54443 Å; K-Beta = 1.39225 Å; $K\alpha_2/K\alpha_1$ intensity ratio = 0.500). Data were collected in continuous (gonio) scan mode over a 2θ range of 5.0024° to 74.9684°, using a step size of 0.0260° 2θ and a scan step time of 23.97 s. The instrument operated in θ–θ geometry using a flat sample stage, with a goniometer radius of 240 mm, automatic divergence slit (irradiated length = 4 mm), and specimen length of 10 mm. The measurement temperature was 25 °C and no incident beam monochromator was employed. The diffractometer model number is 0000000011078671 (EMPYREAN system, NGRL Flat Programme) and the system was operated under the NGRL Flat Programme configuration.

Prior to analysis, each rock sample was disaggregated and ground to below 270 mesh (~53 µm) using a Spex mixer mill with a steel grinding container and ball, following the standard NGRL preparation protocol. The grinding duration was adjusted for each sample according to hardness, typically between five and eight minutes. Ground powders were transferred to weighing paper and sieved to verify particle size. Powders were then back-loaded into flat aluminium sample holders and lightly pressed to present a smooth, level surface, with attention given to minimising preferred orientation of platy phyllosilicate grains. Phase identification was performed by matching observed peak positions (2θ), d-spacings (Å), and relative intensities against reference patterns in the International Centre for Diffraction Data (ICDD) Powder Diffraction File (PDF) database using HighScore Plus software (PANalytical). Mineral identifications were accepted only where at least three diagnostic peaks were confirmed in the correct relative intensity ratios for each phase.

Table 1: Geographic coordinates, elevations, and field descriptions of the rock samples collected from the Jiko abandoned mine site.

DOI: https://doi.org/10.57233/ijsgs.v12i1.1060 ISSNp: 2488-9229; ISSNe: 3027-1118

IJSGS FUGUSAU VOL. 12(1) WEBSITE: https://fugus-

Sample	Latitude (N)	Longitude (E)	Elev. (m ASL)	Field Description
R1	09°39′55.33″	006°49′01.4″	398	Medium-grey phlogopite–quartz schist; moderate schistosity; quartz veins ≤2 cm
R2	09°40′12.1″	006°49′05.8″	375	Light-grey to brownish mica schist; well-defined foliation; Fe-oxide staining along cleavage
R2B	09°39′54.7″	006°49′02.5″	391	Grey-brown schistose rock; moderate alteration; limonite-stained surfaces; foliation dips ~55° NE
R3	09°39′54.3″	006°49′04.0″	398	Dark grey phlogopite schist with Ti-bearing accessory phases; massive quartz lenses; faint metallic lustre
R3B	09°40′12.1″	006°49′05.8″	375	Gneissic rock; alternating felsic–mafic bands ~5–15 mm; pervasive Fe-oxide coating on fracture surfaces
R4	09°39′56.0″	006°49′01.6″	372	Pale grey phlogopite–albite schist; relatively fresh; strong schistosity; minor quartz stringers

3.3 Optical Petrography of Thin Sections

Representative samples were prepared as standard petrographic thin sections at the NGSA Petrology Laboratory, Kaduna. Rock billets were cut from fresh interiors of hand specimens using a diamond saw, oriented to include the principal foliation where present, then mounted on standard glass slides using epoxy resin and ground progressively to the conventional petrographic thickness of approximately 30 µm. Sections were cover-slipped with Canada Balsam for permanent preparation.

All sections were examined systematically under a polarising petrographic microscope (Olympus Model) in the Department of Geology, Federal University of Technology, Minna, Nigeria, using plane-polarised light (PPL) and cross-polarised light (XPL) at nominal magnifications of ×40, ×100, and ×400 (objective lenses ×4, ×10, and ×40 with ×10 eyepiece). Mineral identification relied on standard optical features, including colour and pleochroism in PPL, birefringence and interference colours in XPL, extinction angle, cleavage traces, habit, crystal form, and grain-boundary relationships. The standard reference texts of El Mendili*et al.*, 2019 &Maestracci*et al.*, 2023 were employed for mineral identification. Particular attention was directed at fabric characterisation (e.g., foliation, banding, lineation), textural features (e.g., lepidoblastic, granoblastic, porphyroblastic), grain-boundary types, alteration textures (e.g., sericitisation, chloritisation, Fe-oxide replacement), and paragenetic relationships between primary and secondary mineral phases. Because reflected-light ore microscopy was not available for this study, opaque phases were characterised in transmitted light only by their habit, colour in transmitted light where possible, and by cross-referencing with XRD identifications.

4.0 RESULTS

4.1 Bulk Mineralogy by X-Ray Diffraction (XRD)

4.1.1 General Phase Assemblage

Powder XRD analysis of the six rock samples from the Jiko mine site identified a recurring primary assemblage dominated by quartz, phlogopite, and albite, with secondary and accessory phases including ilmenite, goethite, and haematite distributed differentially across the sample set (Tables 2 and 3, and Figures 2-6). Phase identification followed the criterion of at least three confirmed diagnostic peaks per mineral in the correct relative intensity ratios. Diffractograms for all samples share a characteristic set of strong quartz peaks and a prominent low-angle phlogopite basal reflection, indicating that quartz and phlogopite are the two most consistently expressed and volumetrically abundant mineral constituents across all analysed samples. Albite was confirmed in five of the six samples. Secondary Fe-oxyhydroxide and Fe-oxide phases are absent or present only as traces in the freshest samples (R1, R4) and increase in clarity and peak intensity in the more altered samples (R2B, R3B).

4.1.2Quartz

Quartz (SiO_2) is identified in all six samples as a major phase by its three principal reflections: a strong peak at approximately 20.86° 2θ corresponding to the (100) d-spacing of 4.26 Å, a very strong and diagnostic peak at 26.64° 2θ (d = 3.34 Å, the (011) reflection), and a moderate peak at 50.13° 2θ (d = 1.82 Å). These peaks are sharp and narrow in the freshest samples (R1, R4), indicating well-crystallised, coarse-grained quartz. In the more altered samples (R2B, R3B), the quartz peaks remain sharp and intense but are superimposed on a slightly elevated background, reflecting the co-precipitation of poorly crystalline Fe-oxide phases. No evidence of cristobalite or tridymite polymorphs was detected. The consistent presence of sharp quartz reflections confirms that quartz is stable and unaffected by the degree of alteration observed in these samples.

4.1.3 Phlogopite

Phlogopite [$KMg_3(AlSi_3O_{10})(OH)_2$], the dominant mica phase, is confirmed in all six samples by a series of characteristic reflections. The most diagnostic is the strong basal (001) reflection at approximately 8.84° 2θ, corresponding to a d-spacing of 10.00 Å, which represents the characteristic layer-to-layer spacing of a 10 Å mica. This reflection is very strong in the freshest samples (R1, R3, R4) and remains clearly expressed even in the most altered sample (R3B), though its relative intensity decreases slightly, consistent with partial degradation of the mica interlayer structure. Additional confirmatory peaks include the (002) basal reflection at 17.78° 2θ (d = 4.98 Å), the combined (112)/(006) region near 26.65° 2θ (d = 3.34 Å, overlapping partially with the quartz (011) peak), and the

DOI: https://doi.org/10.57233/ijsgs.v12i1.1060 ISSNp: 2488-9229; ISSNe: 3027-1118

IJSGS FUGUSAU VOL. 12(1) WEBSITE: https://fugus-

(113) reflection at approximately 28.12° 2θ (d = 3.17 Å), which is most clearly expressed in the freshest samples R1 and R4. The persistence of strong phlogopite basal reflections at 10.00 Å across all samples confirms that the mica interlayer remains intact and that no significant smectitisation or illitisation of phlogopite has occurred, consistent with the low-grade nature of chemical alteration inferred from field and petrographic observations.

Table 2: Identified mineral phases, principal XRD peak positions (2θ), d-spacings, and relative intensities for all analysed rock samples from Jiko.

Sample	Mineral Assemblage	Principal 2θ Peaks (°)	d-spacing (Å)	Relative Intensity (Counts)
R1	Quartz	20.86, 26.64, 50.13	4.26, 3.34, 1.82	Strong, Very Strong, Moderate
	Phlogopite	8.84, 17.78, 26.65, 28.12	10.00, 4.98, 3.34, 3.17	Very Strong, Moderate, Strong, Moderate
	Albite	21.98, 27.91, 43.78	4.04, 3.19, 2.06	Moderate, Moderate, Weak
R2	Quartz	20.86, 26.64, 50.13	4.26, 3.34, 1.82	Strong, Very Strong, Moderate
	Phlogopite	8.84, 17.78, 26.65	10.00, 4.98, 3.34	Strong, Moderate, Strong
	Albite	21.98, 27.91	4.04, 3.19	Weak, Moderate
	Goethite (incipient)	21.21, 33.20	4.18, 2.69	Weak, Weak
R2B	Quartz	20.86, 26.64, 50.13	4.26, 3.34, 1.82	Strong, Very Strong, Moderate
	Phlogopite	8.84, 17.78, 26.65	10.00, 4.98, 3.34	Very Strong, Moderate, Strong
	Albite	21.98, 27.91	4.04, 3.19	Moderate, Moderate
	Goethite	21.21, 33.20, 36.62	4.18, 2.69, 2.45	Moderate, Moderate, Weak
	Haematite	33.15, 35.64, 40.85	2.70, 2.52, 2.20	Moderate, Moderate, Weak
R3	Quartz	20.86, 26.64, 50.13	4.26, 3.34, 1.82	Strong, Very Strong, Moderate
	Phlogopite	8.84, 17.78, 26.65	10.00, 4.98, 3.34	Very Strong, Strong, Strong
	Ilmenite	23.94, 32.47, 48.73	3.71, 2.75, 1.86	Moderate, Strong, Moderate
	Goethite (trace)	21.21	4.18	Weak
R3B	Quartz	20.86, 26.64, 50.13	4.26, 3.34, 1.82	Strong, Very Strong, Moderate
	Phlogopite	8.84, 17.78, 26.65	10.00, 4.98, 3.34	Moderate, Weak, Moderate
	Albite	21.98, 27.91	4.04, 3.19	Weak, Weak
	Goethite	21.21, 33.20, 36.62	4.18, 2.69, 2.45	Strong, Moderate, Moderate
	Haematite	33.15, 35.64, 40.85	2.70, 2.52, 2.20	Strong, Strong, Moderate
R4	Quartz	20.86, 26.64, 50.13	4.26, 3.34, 1.82	Strong, Very Strong, Moderate
	Phlogopite	8.84, 17.78, 26.65, 28.12	10.00, 4.98, 3.34, 3.17	Very Strong, Strong, Very Strong, Moderate
	Albite	21.98, 27.91, 43.78	4.04, 3.19, 2.06	Moderate, Strong, Weak
	Goethite (trace)	21.21	4.18	Weak

Table 3: Summary of mineral phase occurrence across the six Jiko rock samples. *✓✓✓ = abundant; ✓✓ = moderate; ✓ = minor; tr = trace; — = absent.*

Mineral	R1	R2	R2B	R3	R3B	R4
Quartz	✓✓✓	✓✓✓	✓✓✓	✓✓✓	✓✓✓	✓✓✓
Phlogopite	✓✓✓	✓✓	✓✓✓	✓✓✓	✓✓	✓✓✓
Albite	✓✓	✓	✓✓	—	✓	✓✓
Ilmenite	—	—	—	✓✓	—	—
Goethite	—	✓	✓✓	tr	✓✓✓	tr
Haematite	—	—	✓✓	—	✓✓✓	—
Alteration grade	**Fresh**	**Slight**	**Moderate**	**Fresh–slight**	**Moderate–strong**	**Fresh**

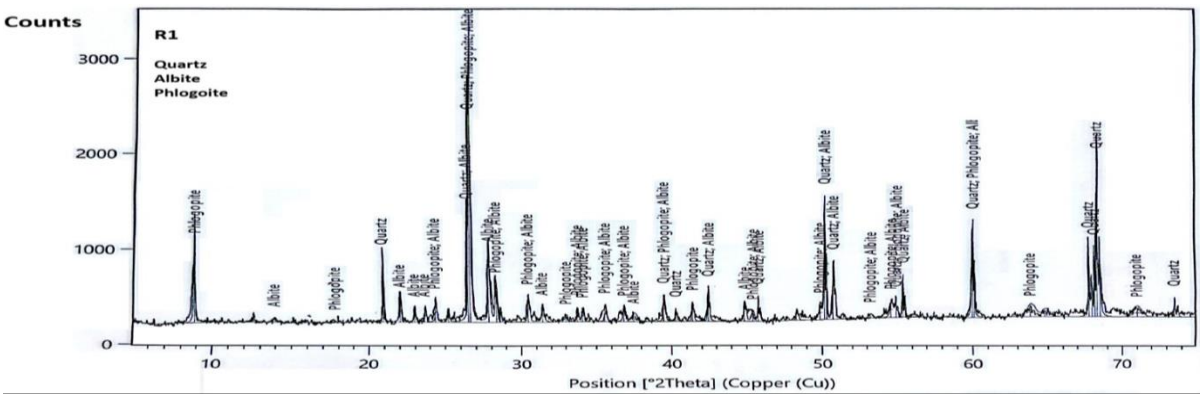

DOI: https://doi.org/10.57233/ijsgs.v12i1.1060 ISSNp: 2488-9229; ISSNe: 3027-1118

Figure 2: Diffractogram of sample R1 showing identified peaks for quartz, phlogopite and albite as the primary mineral phases in Jiko basement rock.

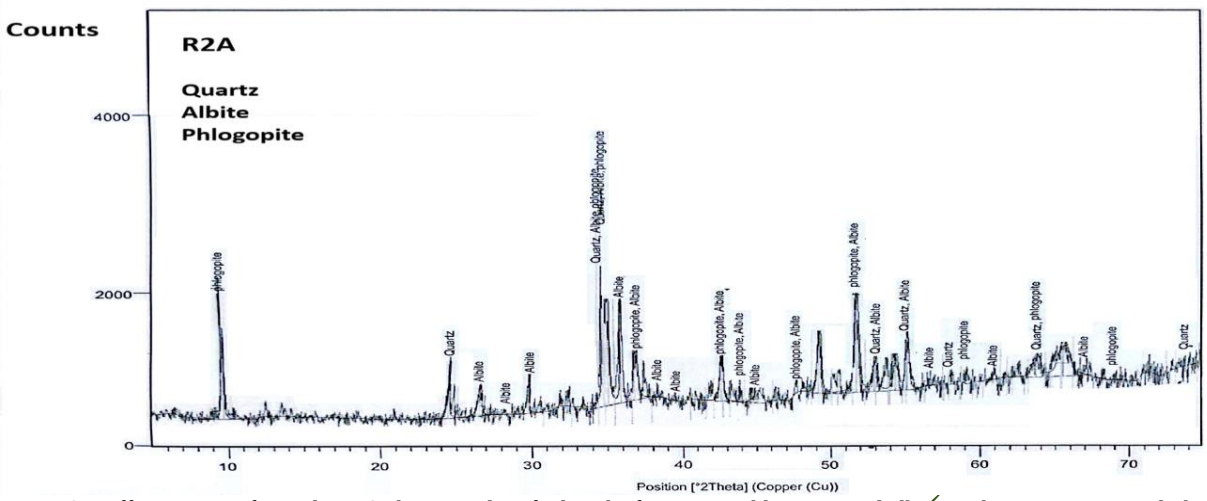

Figure 3: Diffractogram of sample R2A showing identified peaks for quartz, phlogopite and albite as the primary mineral phases in Jiko basement rock.

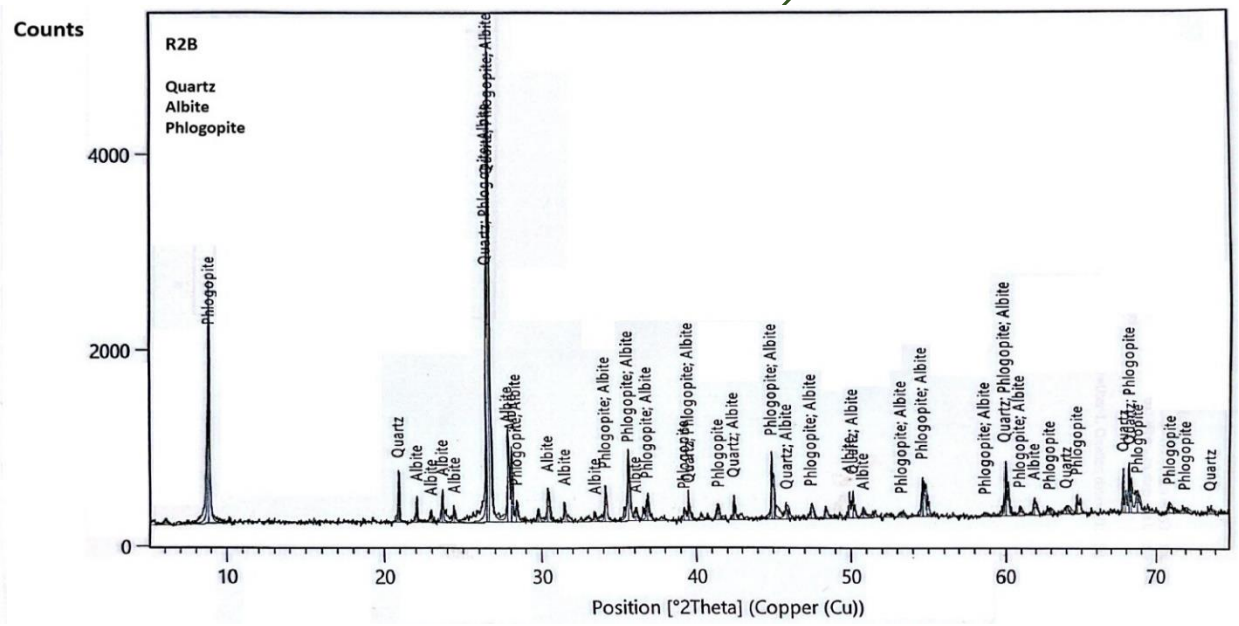

Figure 4: Diffractogram of sample R2B showing identified peaks for quartz, phlogopite and albite as the primary mineral phases in Jiko basement rock.

DOI: https://doi.org/10.57233/ijsgs.v12i1.1060 ISSNp: 2488-9229; ISSNe: 3027-1118
IJSGS FUGUSAU VOL. 12(1) WEBSITE: https://fugus-

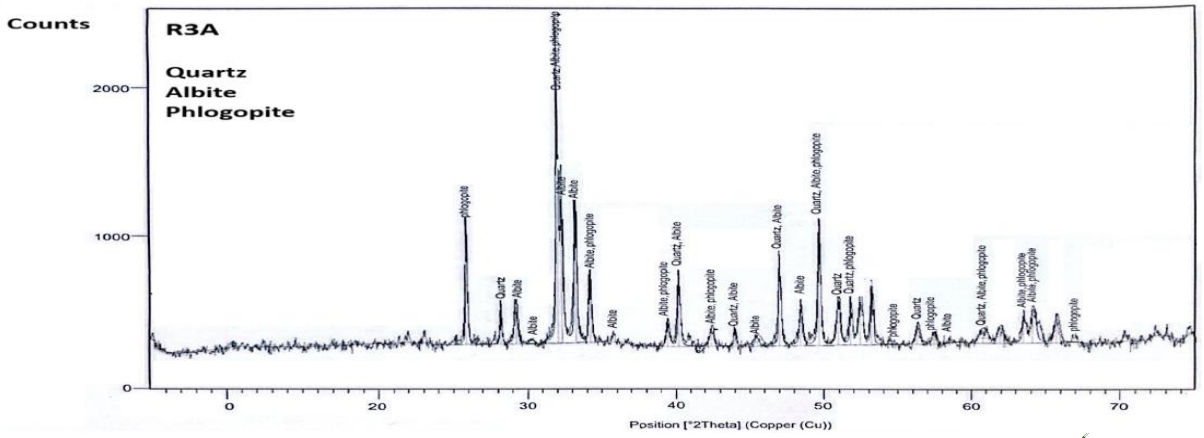

Figure 5: Diffractogram of sample R3A showing identified peaks for quartz, phlogopite and albite as the primary mineral phases in Jiko basement rock.

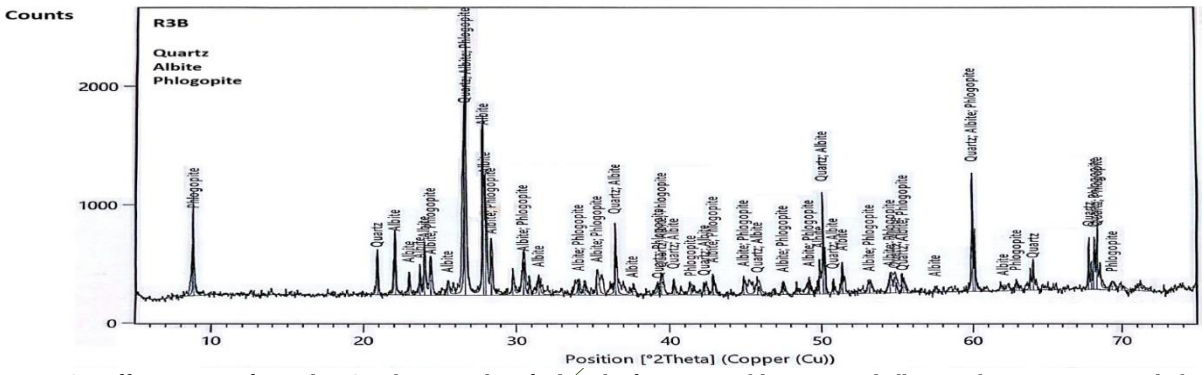

Figure 6: Diffractogram of sample R3B showing identified peaks for quartz, phlogopite and albite as the primary mineral phases in Jiko basement rock.

4.1.4 Albite

Albite ($NaAlSi_3O_8$; low albite), the sodic plagioclase feldspar, is confirmed in all samples. Diagnostic peaks include a moderate reflection near 21.98° 2θ (d = 4.04 Å), a moderate to strong peak at 27.91° 2θ (d = 3.19 Å), and a weaker peak at 43.78° 2θ (d = 2.06 Å). In the freshest samples (R1, R4), the albite peaks are clear and moderately intense, whereas in the more altered samples (R2, R2B, R3B) the albite reflections are weaker, consistent with partial dissolution or replacement of the feldspar framework during hydrolytic weathering. The absence of albite peaks in sample R3 is noteworthy and corresponds to the same sample that exhibits ilmenite and the darkest, most mafic hand-specimen character; this suggests that R3 may represent a more mica-oxide-rich and feldspar-depleted lithological variant, possibly reflecting compositional differences in the protolith or greater replacement of feldspar by secondary phases.

4.1.5 Ilmenite

Ilmenite ($FeTiO_3$) is identified exclusively in sample R3, where it produces three clear reflections: a moderate peak at 23.94° 2θ (d = 3.71 Å, the (006) reflection), a strong peak at 32.47° 2θ (d = 2.75 Å, the (110) plane), and a moderate peak at 48.73° 2θ (d = 1.86 Å, the (116) plane). These peaks match the reference pattern for ilmenite (ICDD PDF card no. 29-0733) with high confidence. The ilmenite reflections are absent from all other samples, indicating a localised occurrence of this Ti-Fe oxide phase. The presence of ilmenite in R3 is consistent with its notably dark colour and greater density in hand specimen. Ilmenite is a common accessory mineral in medium- to high-grade metamorphic rocks and in Fe-Ti-enriched basement lithologies, and its occurrence in this context suggests a protolith or source component enriched in Fe and Ti relative to the surrounding mica schists.

4.1.6 Goethite and Haematite

Goethite (α-FeOOH) and haematite (α-Fe_2O_3) are identified as secondary, alteration-derived phases in samples R2, R2B, R3, and R3B. In sample R2, only trace goethite is detected, with weak reflections at 21.21° 2θ (d = 4.18 Å, the (110) reflection) and 33.20° 2θ (d = 2.69 Å, the (130) reflection), confirming incipient oxidative weathering. In sample R2B, goethite peaks are clearly expressed at 21.21°, 33.20°, and 36.62° 2θ (d = 4.18, 2.69, and 2.45 Å respectively), and are accompanied by haematite peaks at 33.15° 2θ (d = 2.70 Å), 35.64° 2θ (d = 2.52 Å), and 40.85° 2θ (d = 2.20 Å). In sample R3B, which represents the most altered sample, both goethite and haematite peaks are strong and clearly resolved, with haematite reflections at 33.15°, 35.64°, and 40.85° 2θ being among the most intense

DOI: https://doi.org/10.57233/ijsgs.v12i1.1060 ISSNp: 2488-9229; ISSNe: 3027-1118

secondary phase peaks in the entire dataset. The detection of haematite alongside goethite in the more altered samples is significant, as haematite typically forms from dehydration of goethite under warmer, seasonally drier conditions, suggesting that these samples have undergone repeated wetting-drying cycles during exposure at or near the ground surface. A trace goethite reflection at 21.21° 2θ is also present in the otherwise fresh sample R3, attributed to a minor surface oxidation film rather than pervasive alteration.

4.2 Optical Petrography

4.2.1 General Fabric and Texture

Petrographic examination of the thin sections reveals two well-defined fabric domains - the schistose domain and the gneissic to altered domain - each characterised by distinctive mineral assemblages, grain sizes, textural relationships, and degrees of alteration (Table 4, Figures 7-8). These domains correspond directly to the two main hand-specimen assemblages identified in the field.

Table 4: Summary of key petrographic features observed in the two rock domains identified at the Jiko abandoned mine site.

Feature	Schistose Domain (R1, R2, R4)	Gneissic / Altered Domain (R2B, R3, R3B)
Macroscopic fabric	Well-defined schistosity; aligned mica laths; platy parting parallel to S_1 foliation	Compositional gneissic banding; alternating felsic–mafic layers 5–15 mm thick
Grain size	Fine- to medium-grained (0.2–1.5 mm); lepidoblastic to granoblastic texture	Medium- to coarse-grained (0.5–3.0 mm); granoblastic to porphyroblastic texture
Quartz habit	Anhedral to subhedral elongate ribbons; undulose extinction; sutured grain boundaries	Subhedral to anhedral equant grains; polygonal boundaries locally; patchy extinction
Phlogopite/biotite habit	Subhedral to euhedral lath-shaped crystals defining S_1; strong pleochroism pale yellow-brown to dark reddish-brown in PPL; parallel extinction in XPL	Lath-shaped to irregular; more fractured and kinked; darker brown to opaque cores; frayed terminations more developed
Alteration features	Frayed mica cleavage-plane margins; incipient feldspar sericitisation; mild dusty turbidity	Advanced feldspar turbidity; pervasive sericitic replacement; Fe-oxide coatings on grain boundaries and fractures
Secondary phases	Minimal to absent; rare trace Fe-oxide along micro-fractures	Fe-oxide precipitates (goethite/haematite) along fractures, foliation planes, and intergranular boundaries

4.2.2 Schistose Domain (Samples R1, R2, R4)

In plane-polarised light (PPL), thin sections of the schistose rocks immediately reveal a strong preferred fabric defined by the alignment of elongate, platy mica laths (~0.3–1.5 mm in length) parallel to the principal foliation (S_1). The mica crystals display the characteristic pleochroism of phlogopite and biotite, ranging from pale straw yellow to medium brown in PPL when observed parallel to the cleavage, and deepening to a rich reddish-brown when the vibration direction is perpendicular to cleavage. This strong pleochroic scheme, with absorption Z > Y > X, is diagnostic of trioctahedral micas and consistent with phlogopite or Mg-Fe biotite, in agreement with the XRD identification. Individual mica crystals are subhedral to euhedral lath-shaped, with well-defined (001) basal cleavage traces visible as fine parallel lines along the length of each crystal. In cross-polarised light (XPL), the micas display high second-order birefringence interference colours (bright yellows, oranges, and pinks), parallel to near-parallel extinction, and occasional bird's-eye extinction when viewed perpendicular to the c-axis. Some mica laths show kinked or slightly bent cleavage traces in the more deformed portions of the sections, indicating that post-crystallisation strain was accommodated within the mica fabric.

Figure 7: Photomicrograph of rock sample from L4 at Jiko under PPL and XPL (Magnification = x10).

DOI: https://doi.org/10.57233/ijsgs.v12i1.1060 ISSNp: 2488-9229; ISSNe: 3027-1118
IJSGS FUGUSAU VOL. 12(1) WEBSITE: https://fugus-

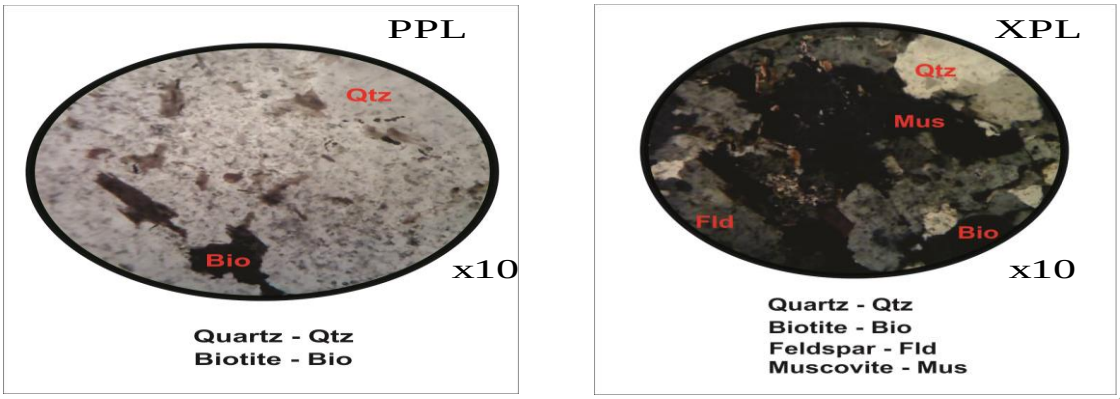

Figure 8 : Photomicrograph of rock sample from L5 at Jiko under PPL and XPL (Magnification = x10).

Quartz in the schistose domain occurs as anhedral to subhedral grains and elongate ribbons (~0.2-0.8 mm) aligned parallel to the foliation between the mica-rich layers. In PPL, quartz is colourless and isotropic in appearance, while in XPL it displays characteristic low-order grey to white interference colours (first-order white). Widespread undulose extinction, whereby the extinction position sweeps gradually across individual grains rather than switching sharply, is consistently observed in quartz grains throughout sections R1, R2, and R4, indicating that the quartz has been subjected to crystal-plastic deformation under stress. Sutured grain boundaries, where the contacts between adjacent quartz grains show irregular interlocking embayments, are developed in samples R1 and R4, suggesting that grain-boundary migration recrystallisation has occurred. Rare subgrain boundaries are visible in some quartz ribbons under XPL as narrow internal extinction boundaries that subdivide a single grain into slightly misoriented domains.

Feldspar (albite) is present in the schistose sections as anhedral to subhedral grains (~0.3-1.0 mm) dispersed among the mica and quartz domains. In PPL, feldspar grains are generally colourless to pale grey, with a distinctive dull, dusty appearance in samples R2 compared to the cleaner, more transparent grains in R1 and R4. In XPL, albite is identified by its characteristic polysynthetic twinning (albite law), expressed as closely spaced parallel twin lamellae that produce alternating extinction positions under rotating crossed polarisers. The birefringence is low (first-order grey to white), consistent with albite feldspar. In sample R2, many feldspar grains show incipient sericitisation, expressed as a finely distributed dusty to scaly white mica (sericite) alteration product coating the interior and particularly the core regions of grains. Under high magnification (×400), these alteration products appear as very fine-grained, random-orientation muscovite-group minerals replacing the original albite framework. This sericitisation represents the earliest microscale stage of feldspar hydrolytic breakdown.

A particularly diagnostic alteration texture observed in the schistose sections is the occurrence of frayed, ragged, or comb-like margins on phlogopite/biotite laths, especially in sample R2. Under PPL, the edges of affected mica crystals show irregular, fringed terminations that lack the sharp, planar cleavage boundaries typical of intact mica. Under XPL, the fringed margins show a reduction in birefringence and a mottled interference colour pattern, distinguishable from the bright, clean colours of the intact crystal interior. These frayed margins are interpreted as zones of incipient oxidative and hydrolytic attack along structurally weak (001) cleavage planes, where K^+ and Fe^{2+}/Mg^{2+} are most susceptible to leaching by infiltrating pore water. In R1 and R4, mica margins are clean, sharp, and unfrayed, indicating that these samples have experienced minimal chemical attack at the grain scale.

4.2.3 Gneissic to Altered Domain (Samples R2B, R3, R3B)

The gneissic sections are coarser grained overall (~0.5–3.0 mm) and display a pronounced compositional banding visible at the thin-section scale. Felsic bands consisting of quartz and feldspar alternate with darker mafic bands dominated by biotite/phlogopite, reproducing at the microscale the hand-specimen banding described in the field. The transition between felsic and mafic bands is generally sharp, occurring over one to two grain diameters.

Quartz in the gneissic sections (R2B, R3, R3B) forms equant to slightly elongate anhedral grains with polygonal grain boundaries and triple-junction geometry in the more recrystallised regions, indicative of granoblastic texture formed under static annealing conditions. Undulose extinction remains present but is less pervasive than in the schistose domain. In sample R3B, quartz grains in proximity to Fe-oxide-bearing fractures show a pale brownish tint in PPL attributed to fine inclusions or surface coatings of Fe-oxide, distinguishable from the clean, colourless quartz in unaffected regions of the same section.

The mica component in the gneissic sections is more heterogeneous than in the schistose domain. In sample R3, the mica crystals are generally intact and show the same strong pleochroism as in the schistose sections, but with a noticeably darker, more opaque character under PPL at high magnification, consistent with a more Fe-rich trioctahedral mica composition. Individual mica laths in R3 are larger (up to 3 mm) and show a stronger concentration in the mafic bands. In contrast, micas in samples R2B and R3B are more strongly altered: they are darker in PPL, show irregular and

DOI: https://doi.org/10.57233/ijsgs.v12i1.1060 ISSNp: 2488-9229; ISSNe: 3027-1118

cracked cleavage traces under XPL, and have cores that are markedly less transparent than those of R1 and R4, suggesting progressive Fe-oxidation within the mica lattice. Some mica grains in R3B show partial replacement by iron oxide in their cores and along intergranular boundaries, creating a characteristic pseudomorphic replacement texture in which the mica crystal form is broadly preserved but the optical properties of the interior are partially masked by opaque to dark-brown Fe-oxide pigmentation.

In sample R3, ilmenite is identified in thin section as small (~0.05-0.2 mm), highly opaque, sub-rounded to anhedral grains with a very faint brownish tint at their margins in transmitted PPL where the grains are thin enough to permit slight transmission. These grains occur as inclusions within phlogopite laths and as interstitial grains at mica-quartz boundaries, consistent with an accessory mineral that crystallised in equilibrium with the mica assemblage during metamorphism. Cross-referencing with the XRD identification of ilmenite by its characteristic strong peak at 32.47° 2θ confirms these opaque grains as ilmenite rather than magnetite or pyrite.

The most conspicuous alteration feature of the gneissic sections is the pervasive development of iron oxide coatings and precipitates along fractures, cleavage planes, and intergranular boundaries. In PPL, these appear as reddish-brown to dark brown opaque to sub-opaque films, varying from very thin coatings (<0.01 mm) on grain surfaces to thicker (0.1-0.5 mm) irregular infiltrations filling micro-fractures. Under XPL, they are generally extinct or near-extinct, confirming their optically isotropic and amorphous to poorly crystalline nature, consistent with goethite and haematite as identified by XRD. In the most altered sample, R3B, these Fe-oxide precipitates form a near-continuous network along foliation planes and grain boundaries, effectively sealing the original interstitial pore space. The concentration of Fe-oxide coatings along fractures in R2B and R3B provides direct microscopic evidence that iron-bearing fluids migrated preferentially along structurally controlled permeability pathways during weathering.

5.0 DISCUSSION

5.1 Rock Type, Metamorphic Grade, and Lithological Affinity

The integrated XRD and petrographic dataset conclusively characterises the Jiko basement rocks as phlogopite-quartz-albite schists and gneisses of the Precambrian Nigerian Basement Complex, representing metasedimentary and possibly meta-igneous protoliths subjected to low- to medium-grade regional metamorphism.The latter interpretation is supported by the silica versus total alkali (TAS) diagram derived from the major oxide geochemical data reported for the same rock samples by Rasheed *et al.* (2026, in press), as presented in Figure 9 and Table 5. The TAS diagram (Figure 9) provides important constraints on the protolith composition of the basement rocks in the study area.

The presence of phlogopite as the dominant mica phase is particularly diagnostic. Phlogopite, the trioctahedral Mg-end member of the biotite–phlogopite series [$KMg_3(AlSi_3O_{10})(OH)_2$], is characteristic of metamorphosed Mg-rich pelitic or carbonatic protoliths, and its occurrence at Jiko is consistent with the mineral assemblages described from the KusherikiPsammite Formation and related schist belt lithologies of the Minna Sheet 164 region, where phlogopite is among the chief minerals reported alongside quartz, paragonite, muscovite, kyanite, and rutile (Truswell & Cope, 1963; Muhammed *et al.*, 2018). The persistence of strong phlogopite (001) basal reflections at d = 10.00 Å in the XRD patterns of all six samples, coupled with the classic high-birefringence, strong-pleochroism optical properties of the mica observed in thin section, leave no ambiguity in the phase identification.

Table 5: Major element geochemistry of rock samples from the Jiko abandoned mine site determined by ED-XRF spectrometry (values in wt.%). Data from Rasheed *et al.* (2026, in press).

Oxides (wt%)	R1	R2	R2B	R3	R3B	R4	Average
SiO_2	59.30	58.50	63.14	50.64	64.15	60.20	59.32
Al_2O_3	15.78	16.21	15.76	15.84	15.77	15.21	15.76
CaO	6.77	7.10	5.50	6.76	4.86	5.21	6.03
MgO	2.14	2.00	1.28	2.32	1.21	1.34	1.72
K_2O	0.48	0.45	0.90	1.41	0.12	0.16	0.59
Na_2O	1.32	1.29	1.10	1.89	0.37	0.40	1.06
TiO_2	1.59	1.61	1.64	3.09	2.66	2.40	2.17
MnO	0.10	0.12	0.079	0.16	0.058	0.061	0.10
Fe_2O_3	9.51	9.43	9.34	12.36	8.85	8.0	9.58
LOI	1.20	1.00	1.00	1.32	1.31	0.90	1.12

DOI: https://doi.org/10.57233/ijsgs.v12i1.1060 ISSNp: 2488-9229; ISSNe: 3027-1118
IJSGS FUGUSAU VOL. 12(1) WEBSITE: https://fugus-

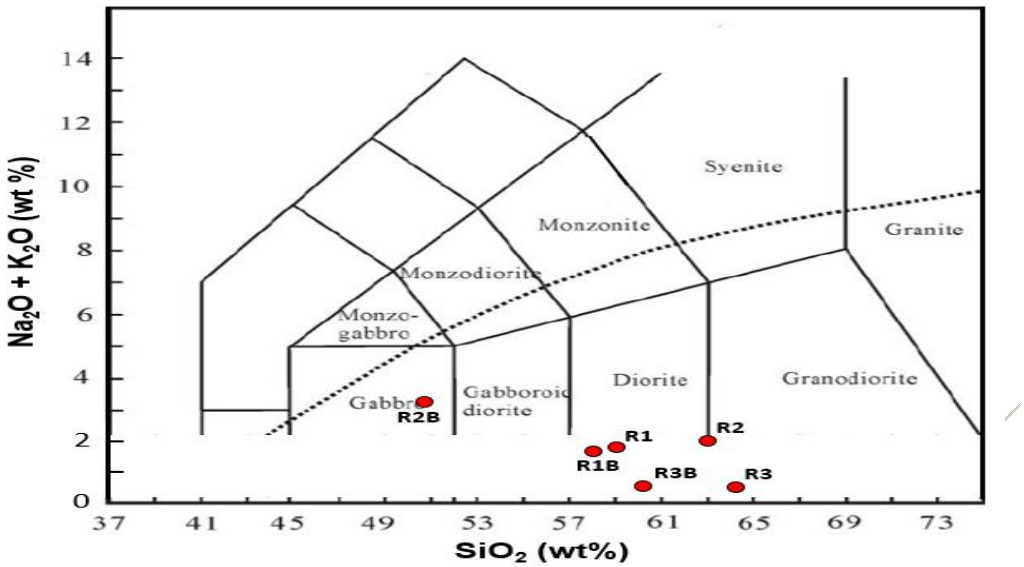

Figure 9: Total alkali versus silica (TAS) diagram showing the classification of sampled rocks from the abandoned Jiko mine site. The diagram illustrates the precursor (protolith) for the basement rocks in the area.

The assemblage quartz + phlogopite + albite, with accessory ilmenite in the Ti-richer samples, is broadly compatible with amphibolite-facies to upper greenschist-facies metamorphic conditions. This interpretation is further supported by the elevated TiO_2 content (mean = 2.17 wt.%) reported for the same rock samples by Rasheed *et al.* (2026, in press), indicating consistency between the mineralogical observations and major oxide geochemical data. The development of a strong S_1 foliation defined by aligned mica laths and deformed quartz ribbons with undulose extinction and sutured grain boundaries indicates that the rocks have experienced significant crystal-plastic deformation, consistent with the Pan-African orogenic reworking that affected the Nigerian Basement Complex between approximately 700 and 550 Ma (Ominigbo, 2022). The granoblastic texture and polygonal quartz grain boundaries observed in the gneissic sections suggest that some static recrystallisation or annealing followed the main deformation event. These textural observations parallel those reported by Muhammed *et al*. (2018) for mica schists near Kuta, approximately 40 km to the east of Jiko, where a NE-SW structural trend and similar phlogopite-bearing mineral assemblages were documented within the same Precambrian schist belt.

5.2 Significance of Quartz as a Framework Mineral

Quartz is the most consistently expressed phase in the XRD data of all six samples and is confirmed petrographically as the principal framework-forming silicate. Its very strong (011) reflection at 26.64° 2θ (d = 3.34 Å) is the most intense peak in every diffractogram and serves as the primary diagnostic reflection. The stability and sharpness of quartz peaks across both fresh and altered samples confirm that quartz is chemically inert under the weathering conditions prevailing at Jiko, acting as a passive diluent rather than contributing to secondary mineral formation. Petrographically, the undulose extinction, sutured grain boundaries, and subgrain development in quartz indicate that the rocks experienced crystal-plastic deformation, probably during the main Pan-African compressional event. Quartz ribbons aligned parallel to the foliation in the schistose sections are a particularly reliable indicator of high finite strain accumulated during prograde metamorphism. The concentration of quartz into discrete elongate lenses and ribbons alternating with mica-rich layers reflects the operation of metamorphic differentiation and pressure-solution processes that segregated SiO_2-rich and mica-rich domains during deformation.

5.3 Phlogopite and Albite as Primary Repositories for Trace Elements

Among the identified primary mineral phases, phlogopite and albite are most relevant to the geochemical behaviour of trace metals at Jiko. Trioctahedral micas are known to accommodate a wide range of divalent and trivalent cations by coupled substitution in both octahedral and interlayer sites. In phlogopite, Mg^{2+} in the octahedral sheet can be substituted by Fe^{2+}, Mn^{2+}, Ni^{2+}, and Pb^{2+} (within structural limits), while the interlayer K^+ site can accommodate Rb^+, Cs^+, and Ba^{2+}. The frayed mica margins and incipient cleavage-plane alteration observed in petrographic sections R1 and R2 indicate that these substitution-enriched mica grains are already beginning to release lattice-bound constituents along structurally weak cleavage domains. The moreopaque, Fe-rich mica cores observed in sections R3 and R3B further suggest progressive oxidation of Fe^{2+} within the mica octahedral sheet to Fe^{3+}, a process that destabilises the mica structure and promotes leaching of associated divalent cations (Li et al. 2022).

Albite feldspar, confirmed by its characteristic polysynthetic twinning in XPL and diagnostic XRD peaks at 21.98°, 27.91°, and 43.78° 2θ, provides an additional structural reservoir for trace elements incorporated during metamorphic crystallisation. The incipient sericitisation of albite grains observed in thin sections of R2where fine-

DOI: https://doi.org/10.57233/ijsgs.v12i1.1060 ISSNp: 2488-9229; ISSNe: 3027-1118

grained sericite alteration products partially replace feldspar coresrepresents the first stage of hydrolytic feldspar breakdown, converting the relatively soluble Al-Si framework into a secondary illitic mica while releasing Na^+, Ca^{2+}, and trace metals to pore waters. The progressive weakening and eventual absence of albite peaks in the more altered samples (R3B) corroborates petrographic observations and indicates that feldspar breakdown is more advanced in the gneissic domain, where fluid access along fractures and grain boundaries is enhanced by the more permeable banded fabric.

5.4 Ilmenite as an Indicator of Ti-Fe-Enriched Basement Lithology

The identification of ilmenite ($FeTiO_3$) exclusively in sample R3 by the strong characteristic XRD peak at 32.47° 2θ (d = 2.75 Å) and the accompanying peaks at 23.94° and 48.73° 2θ, corroborated by the presence of small, highly opaque grains with faintly brownish-translucent margins in thin section, establishes that at least one of the sampled lithologies contains a primary Fe-Ti oxide accessory mineral assemblage. Ilmenite in metamorphic rocks typically crystallises as a stable accessory phase during prograde metamorphism of Fe-Ti-enriched pelitic or mafic metavolcanic protoliths, and its occurrence alongside phlogopite is geologically consistent with a mica schist of mafic provenance or with an Fe-Ti-enriched sedimentary protolith. Comparable Ti-bearing mineral assemblages, including rutile and topaz in addition to ilmenite, have been reported in mica schists and quartzites of the Kuta area of Minna Sheet 164 (Muhammed *et al.*, 2018), supporting the interpretation that Ti-enriched basement lithologies are a recurring feature of the north-central Nigerian schist belt.

The absence of ilmenite from the XRD patterns of all other samples suggests either that the ilmenite-bearing lithology is laterally restricted or that the ilmenite content is below XRD detection limits in other samples. The occurrence of ilmenite as inclusions within phlogopite laths in thin section of R3 is consistent with an equilibrium paragenesis in which both minerals crystallised during the same metamorphic event, and it also implies that the ilmenite is protected from rapid oxidative weathering by its mica host. However, the faint brownish rim on some ilmenite grains suggests that the outermost portions are beginning to be oxidised, potentially forming fine-grained leucoxene (amorphous to poorly crystalline TiO_2 ± Fe-hydroxide), a common ilmenite alteration product. This partial alteration may contribute trace Fe to the circulating pore fluids even in the absence of complete ilmenite dissolution.This process is interpreted as representing an intermediate to advanced stage in the conceptual model of lithological control on Pb mobilisation (release and redistribution) proposed by Rasheed *et al.* (in press) for the Jiko area.

5.5 Goethite and Haematite: Secondary Mineral Formation and Paragenetic Significance

The systematic identification of goethite and haematite as secondary phases in the altered samples, and their progressive increase in XRD peak intensity from trace levels in R2 to strong peaks in R3B, provides the mineralogical record of a coherent oxidative weathering sequence. Goethite (α-FeOOH) forms through the oxidation and hydrolysis of Fe^{2+} released during the alteration of phlogopite, biotite, and ilmenite according to reactions involving Fe-bearing mica breakdown in the presence of oxygenated water. The identification of goethite by its diagnostic (110) reflection at 21.21° 2θ (d = 4.18 Å) and confirmatory peaks at 33.20° 2θ (d = 2.69 Å) and 36.62° 2θ (d = 2.45 Å) across the altered samples is consistent with the reddish-brown to yellow-brown surface coatings and Fe-oxide films observed in hand specimens and in thin sections of R2B and R3B.This interpretation is consistent with the elevated Fe_2O_3 content (mean = 9.58 wt.%; Table 5) reported for the same rock samples by Rasheed *et al.* (2026, in press), indicating strong agreement between the major oxide geochemical data and the mineralogical observations.

The co-occurrence of haematite (α-Fe_2O_3) with goethite in R2B and R3B, confirmed by reflections at 33.15° 2θ (d = 2.70 Å), 35.64° 2θ (d = 2.52 Å), and 40.85° 2θ (d = 2.20 Å), indicates that the oxidative weathering process has advanced to a stage where partial dehydration of goethite has occurred. Haematite forms from goethite dehydration:

$[2\ FeOOH \rightarrow Fe_2O_3 + H_2O]$

under warm, seasonally dry conditions, and the co-existence of both phases in the most weathered samples from Jiko is entirely consistent with the alternating wet-season hydration and dry-season desiccation characteristic of the local savanna climate. Petrographically, the reddish-brown to opaque, near-extinct Fe-oxide coatings along grain boundaries and fractures observed in thin sections of R2B and R3B represent this goethite-haematite mineralisation at the grain scale.

From a paragenetic perspective, the mineralogical sequence inferred for the Jiko rocks proceeds, through 3 stages as reported by Rasheed *et al.* (2026, in press), from a primary assemblage of quartz + phlogopite ± albite ± ilmenite (Stage I, low CIA, no secondary phases, represented by R1 and R4) through an early alteration assemblage showing frayed mica margins, incipient feldspar sericitisation, and trace goethite (Stage II, represented by R2) to a more advanced alteration assemblage featuring co-occurring goethite and haematite with strongly altered mica and feldspar textures (Stage III, represented by R2B and R3B). This paragenetic progression is expressed both in the gradual loss of albite intensity in the XRD patterns and in the petrographic transition from clean, optically homogeneous mineral grains with sharp boundaries to increasingly turbid feldspar, frayed mica, and pervasive Fe-oxide-coated grain boundaries. The structural fabric of the rocks, specifically the schistose foliation and the fracture systems oriented at low angles to the foliation, has served as the principal permeability pathway along which oxidising meteoric waters have advanced into the rock, producing the alteration textures documented in this study.

5.6 Comparison with Neighbouring Basement Mineral Assemblages

DOI: https://doi.org/10.57233/ijsgs.v12i1.1060 ISSNp: 2488-9229; ISSNe: 3027-1118

The Jiko mineral assemblages compare closely with those reported from analogous basement lithologies in the surrounding north-central Nigerian Basement Complex. Muhammed *et al.* (2018) documented phlogopite, paragonite, muscovite, quartz, kyanite, topaz, rutile, kaolinite, and magnetite from mica schists in the Kuta area of the same Minna Sheet 164, and quartzite assemblages dominated by quartz, kyanite, topaz, and rutile from the same sheet. The Jiko assemblages of quartz + phlogopite + albite ± ilmenite are a sub-set of this broader range, lacking the Al-silicate minerals kyanite and topaz that characterise the most aluminous metapelitic horizons but sharing the mica-quartz framework. The occurrence of ilmenite at Jiko rather than rutile (as at Kuta) may reflect a lower-temperature or more Fe-rich metamorphic condition, since rutile is more stable than ilmenite at higher temperatures and under oxidising conditions. The schistose and gneissic fabrics, the NE–SW structural trend, and the association with quartz-vein mineralisation documented at Jiko are all features in common with the wider Kusheriki Schist Group, supporting their geological correlation and confirming that Jiko basement rocks are representative of the regional metamorphic basement rather than anomalous outliers.

The secondary mineral assemblage of goethite ± haematite documented at Jiko by both XRD and petrography is also reasonably consistent with the advanced surface weathering of Fe-bearing basement schists in tropical savanna settings, where a lateritic weathering profile is expected above the fresh basement. The absence of kaolinite or other clay minerals in the XRD patterns of the analysed samples indicates that the sampled rocks represent a level below the main clay-forming weathering front, consistent with the relatively fresh to moderately altered hand-specimen character of the collected material. Future sampling of the overlying saprolite and laterite horizon at Jiko would be expected to reveal a progressively more clay- and Fe-oxide-enriched assemblage as the weathering profile is traced upward toward the surface.

6.0 IMPLICATIONS FOR FUTURE RESEARCH

The mineralogical framework established in this study provides a baseline for interpreting alteration processes and lithological controls in the Jiko basement; however, further work is required to resolve mineral-geochemical relationships at higher analytical resolution. Priority should be given to in situ microanalytical techniques such as SEM-EDS and electron probe microanalysis (EPMA) to quantify mineral chemistry, particularly for phlogopite, feldspar, and Fe-Ti oxides. These methods would enable direct assessment of elemental substitution, trace element partitioning, and the role of specific mineral phases as potential hosts or pathways for metal mobilisation (e.g., Deer *et al.*, 2013; Rollinson, 1993; Rasheed *et al.*, 2026, in press).

To better constrain weathering processes, vertical profiling of the regolith from fresh bedrock through saprolite to laterite is recommended, combined with clay-fraction XRD and complementary techniques (e.g., FTIR or thermal analysis) to identify secondary clay minerals not resolved in bulk XRD patterns. Such an approach would allow the progressive transformation of primary silicates into secondary phases to be quantitatively tracked under tropical weathering conditions (de Souza *et al*., 2021; Freitas *et al*., 2024; Borra *et al*., 2022; Annie *et al*., 2025). The structural control on alteration observed in this study warrants targeted investigation through fracture network analysis, fabric quantification, and permeability assessment, potentially coupled with fluid inclusion or stable isotope studies to characterise fluid sources and pathways. This would provide a more rigorous understanding of fluid-rock interaction and the spatial distribution of Fe-oxide mineralisation.

Integration of the mineralogical dataset with trace element geochemistry and isotopic tracing is also essential for constraining the sources, sinks, and mobility pathways of potentially toxic elements within the Jiko system. Although mineralogical characteristics and major and trace element geochemistry have been comprehensively addressed by Rasheed *et al.* (2026a, 2026b, in press), the integration of isotopic analyses remains a critical gap that warrants further investigation. The development of a quantitative paragenetic–weathering model, linking primary mineral assemblages to secondary alteration products, would significantly enhance the transferability of these findings to similar Pan-African basement terrains affected by mining and tropical weathering.

7.0 CONCLUSION

This study presents the first systematic XRD and optical petrographic characterisation of the basement rocks at the Jiko abandoned mine site, North-Central Nigeria. The following principal conclusions are drawn from the mineralogical evidence:

(1) The Jiko basement is underlain by phlogopite–quartz–albite schists and phlogopite-quartz-feldspar gneisses belonging to the Nigerian Precambrian Basement Complex. These rocks are consistent with low- to medium-grade metamorphic equivalents of pelitic to semi-pelitic protoliths, broadly correlative with the Kusheriki Schist Group lithologies of Minna Sheet 164. The strong NE–SW schistosity, crystal-plastic deformation of quartz, and metamorphic mineral assemblages are diagnostic of Pan-African orogenic reworking.

(2) XRD analysis identifies a consistent primary assemblage of quartz, phlogopite, and albite across all six samples, with ilmenite as a significant accessory phase restricted to the darker, Ti-Fe-enriched sample R3. Phlogopite is the volumetrically dominant mica phase, confirmed by a persistent (001) basal reflection at d = 10.00 Å in all diffractograms. Ilmenite is confirmed by three diagnostic reflections, most notably a strong peak at 32.47° 2θ (d = 2.75 Å).

(3) Secondary phases goethite (α-FeOOH) and haematite (α-Fe_2O_3) occur in the more altered

DOI: https://doi.org/10.57233/ijsgs.v12i1.1060 ISSNp: 2488-9229; ISSNe: 3027-1118

samples (R2B, R3B), confirmed by their diagnostic XRD reflection sets. Their progressive increase in peak intensity from trace levels in R2 to strong, clearly resolved reflections in R3B defines a coherent oxidative weathering sequence that reflects the seasonal climate and the structural permeability of the foliated rock fabric.

(4) Optical petrography reveals two fabric domains. In the schistose domain (R1, R2, R4), well-aligned phlogopite laths define a strong S_1 foliation; quartz shows undulose extinction and sutured grain boundaries indicating crystal-plastic deformation; and alteration features are restricted to frayed mica margins and incipient feldspar sericitisation. In the gneissic to altered domain (R2B, R3, R3B), compositional banding is well-developed, mica grains are more fractured and altered, feldspar shows more advanced turbidity, and pervasive Fe-oxide coatings along fractures and grain boundaries document greater weathering advancement.

(5) The paragenetic sequence at Jiko proceeds from a fresh primary silicate assemblage (quartz + phlogopite ± albite ± ilmenite) through incipient alteration (frayed micas, sericitised feldspars, trace goethite) to a more advanced secondary assemblage (co-occurring goethite + haematite with degraded mica and feldspar). Artisanal mining activities have substantially increased the reactive mineral surface area exposed to oxygenated meteoric water, accelerating this weathering progression along foliation planes and fractures.

Future work should incorporate scanning electron microscopy with energy-dispersive spectroscopy (SEM-EDS) to characterise mica and feldspar compositions at the grain scale and to identify additional fine-grained secondary phases, and reflected-light ore microscopy to examine ilmenite alteration products and any residual ore minerals in the mine workings. Raman spectroscopy of the Fe-oxide phases would enable further discrimination between goethite, lepidocrocite, haematite, and poorly crystalline ferrihydrite within the alteration assemblage, thereby refining the interpretation of weathering intensity and environmental metal partitioning at the Jiko site.

ACKNOWLEDGEMENTS

The authors acknowledge the National Geosciences Research Laboratories (NGRL) of Nigerian Geological Survey Agency (NGSA), Kaduna, for conducting the XRD analyses and thin-section preparation. Additional petrographic work was undertaken in the Department of Geology, Federal University of Technology, Minna, Nigeria. Appreciation is extended to NGRL technical staff for XRD data collection and to colleagues who assisted with photomicrograph documentation. This research received no specific grant from funding agencies in the public, commercial, or not-for-profit sectors.

REFERENCES

Adepoju, S. A., Ojo, O. J., Akande, S. O., & Sreenivas, B. (2021). Petrographic and geochemical constraints on petrofacies, provenance and tectonic setting of Upper Cretaceous sandstones, northern Bida Basin, Nigeria. Journal of African Earth Sciences, 174, 104041.

Ahmed, H., Abubakar, Y.I., Danbatta, U.A., 2020. Geological mapping and mineralisation patterns in Niger State, Nigeria. Journal of African Earth Sciences 169, 103908.

Akinola, O. O., &Olorun, O. A. O. (2021).Geochemical trends in weathering profiles and their underlying Precambrian basement rocks in Akure, Southwestern Nigeria. *Journal of Environmental & Earth Sciences, 3*(2), 7–13. https://doi.org/10.30564/jees.v3i2.3308

Ali, A., Chiang, Y. W., & Santos, R. M. (2022). X-ray diffraction techniques for mineral characterization: A review for engineers of the fundamentals, applications, and research directions. *Minerals, 12*(2), 205. https://doi.org/10.3390/min12020205

Ali, A., et al. (2022).*X-ray Diffraction Techniques for Mineral Characterization: A Review.* Minerals, 12, 205.

Borra, C. R., Pontikes, Y., Binnemans, K., & Van Gerven, T. (2022). Mineralogical and geochemical characterization of the Sta. Cruz nickel laterite deposit, Zambales, Philippines. *Minerals, 12*(3), 305. https://doi.org/10.3390/min12030305

de Souza, D. M., Curi, N., Guilherme, L. R. G., Marques, J. J., & Oliveira, L. C. A. (2021). Chemical and mineralogical changes in the textural fractions of quartzite-derived tropical soils along weathering, assessed by portable X-ray fluorescence spectrometry and X-ray diffraction. *Journal of South American Earth Sciences, 112*, 103634. https://doi.org/10.1016/j.jsames.2021.103634

Ekeleme, I. A., Haruna, A. I., Olorunyomi, A. E., Chollom, J. G., &Ochiba, I. E. (2024). Geology and petrography of the Basement Complex rocks of Tsauni and environs, North-Central Nigeria. *International Journal of Geology and Earth Sciences, 10*(1), 21–37. https://doi.org/10.18178/ijges.10.1.21-37

El Mendili, Y., Chateigner, D., Orberger, B., Gascoin, S., Bardeau, J.-F., Petit, S., Duée, C., Le Guen, M., &Pilliere, H. (2019). Combined XRF, XRD, SEM–EDS, and Raman analyses on serpentinized harzburgite: Implications for exploration and geometallurgy. ACS Earth and Space Chemistry, 3(8), 1634–1645.

Fagbohun, B. J., Omitogun, A. A., Ayoola, F. J., &Bamisaiye, O. A. (2025**).** Spatial analysis of gold occurrences in the Zuru Schist Belt, northwest Nigeria. *Geology, Ecology, and Landscapes, 9*(3), 1015–1033. https://doi.org/10.1080/24749508.2024.2373484

Falana, O. A. (2025). Petrography and Mineralogy of Part of the Gold Schist Belt around Esa-Oke and Environs, Southwestern Nigeria. *Mikailalsys Journal of Advanced Engineering International*, *2*(3), 414-426. https://doi.org/10.58578/mjaei.v2i3.7335

Falana, O. A. (2025). Petrography and mineralogy of part of the gold schist belt around Esa-Oke and environs,

DOI: https://doi.org/10.57233/ijsgs.v12i1.1060 ISSNp: 2488-9229; ISSNe: 3027-1118

Southwestern Nigeria. *Mikailalsys Journal of Advanced Engineering International, 2*(3), 414–426. https://doi.org/10.58578/mjaei.v2i3.7335

Freitas, C. A., Horbe, A. M. C., Albuquerque, M. F. S., & Castro, R. T. (2024).Unraveling parent rock and mineral influences in tropical weathering profiles: REE, Nd and Sr isotopic geochemistry. *Minerals, 14*(5), 470. https://doi.org/10.3390/min14050470

Li, X., Zhou, J., Yuan, P., Wang, Q., Deng, L., & Liu, D. (2022). New insight into biotite weathering in the subtropicTongcheng granite regolith, Hubei Province, South China. *Applied Clay Science, 221*, 106518. https://doi.org/10.1016/j.clay.2022.106518

Lukman, L. M., Najime, T., Ogunleye, P. O., Magaji, S., & Caleb, N. K. (2024). *Geology and geochemical characterization of basement rocks around Burumburum area, North Central Basement Complex, Nigeria*. Earth Sciences, 13**(**1), 14–38. https://doi.org/10.11648/j.earth.20241301.13

Maestracci, B., Delchini, S., Chateigner, D., Pilliere, H., Lutterotti, L., &Borovin, E. (2023). Simultaneous combined XRF–XRD analysis of geological samples: A new methodological approach for on-site analysis on New Caledonian Ni-rich harzburgite. Journal of Geochemical Exploration, 252, 107250.

Muhammed, A., Onoduku, U.S., Ako, T.A., 2018. Geological and geochemical characterization of kyanite-bearing rocks around Kuta, part of Minna Sheet 164, North-Central Nigeria. Asian Journal of Geological Research 1(2), 79-100.

Ojo, E. R., et al. (2020).*Mapping of hydrothermal alterations related to gold mineralization within parts of the Malumfashi Schist Belt, North-Western Nigeria.*Journal of African Earth Sciences, 170**,** 103908. https://doi.org/10.1016/j.jafrearsci.2020.103908

Oluyede, K., Ibrahim, G., Danbatta, U., Ogunleye, P., &Klötzli, U. (2021)**.** Field occurrence, petrography and structural characteristics of the basement rocks in the northern part of Kushaka and BirninGwari schist belts, Northwestern Nigeria. *Journal of Natural Sciences Research, 12*(12). https://doi.org/10.7176/JNSR/12-12-02

Oluyede, K., Ibrahim, G., Danbatta, U., Ogunleye, P., &Klötzli, U. (2021). Field occurrence, petrography and structural characteristics of the Basement Complex rocks in the northern part of Kushaka and BirninGwari schist belts, northwestern Nigeria. *Journal of Natural Sciences Research, 12*(12), 11–29. https://doi.org/10.7176/JNSR/12-12-02

Ominigbo, O. E. (2022). *Evolution of the Nigerian Basement Complex: Current status and suggestions for future research*. *Journal of Mining and Geology, 58*(1), 229–236.

Rahaman, M.A.O., Fadiya, S.L., Adekola, S.A., *et al.*, 2019. A revised stratigraphy of the Bida Basin, Nigeria. Journal of African Earth Sciences 151, 67-81.

Rasheed, H., Suleiman, A., Akande, W. G. 2026b. Mineralogical Controls on Lead Mobilisation in a Basement Terrain: Integrated Geochemical and Petrographic Evidence from an Abandoned Mine Site, North-Central Nigeria. American Journal of Innovative Research & Applied Sciences, 2026, 22(3), In press.

Rasheed, H., Suleiman, A., Akande, W.G., 2026a. Heavy metal contamination and ecological risk assessment in soils and surface waters around an abandoned mine site in Jiko Village, North-Central Nigeria. Journal of Geoscience and Environment Protection, In press.

Salawu, N. B., Fatoba, J. O., Adebiyi, L. S., Orosun, M. M., & Dada, S. S. (2021). New insights on the Ife-Ilesha schist belt using integrated satellite, aeromagnetic and radiometric data. *Scientific Reports, 11*, 15314. https://doi.org/10.1038/s41598-021-94813-1

Yusuf, M.-N. O., Abdulmumin, A. G., Adanlawo, A. K., Telejaiye, O. M., Ogbonnaya, I. S., & Idris, U. A. (2026). Investigation of the mineralogy, physical and geochemical properties of Kataeregi red anthill clay for industrial applications. *Journal of Materials Science: Materials in Engineering, 21*, 3. https://doi.org/10.1186/s40712-025-00372-y

Zafar, M., Wasim, M., Ahmad, N., & Iqbal, M. (2025). Application of XRD, SEM–EDX and FTIR techniques for mineral characterization of geological ores. *Radiochimica Acta*. https://doi.org/10.1515/ract-2024-0335